

Super-heavy electron material as metallic refrigerant for adiabatic demagnetization cooling

Yoshifumi Tokiwa, Boy Piening, Hirale S. Jeevan, Sergey L. Bud'ko, Paul C. Canfield, Philipp Gegenwart

Angaben zur Veröffentlichung / Publication details:

Tokiwa, Yoshifumi, Boy Piening, Hirale S. Jeevan, Sergey L. Bud'ko, Paul C. Canfield, and Philipp Gegenwart. 2016. "Super-heavy electron material as metallic refrigerant for adiabatic demagnetization cooling." *Science Advances* 2 (9): e1600835. <https://doi.org/10.1126/sciadv.1600835>.

Super-heavy electron material as metallic refrigerant for adiabatic demagnetization cooling

Yoshifumi Tokiwa,^{1,2,3*} Boy Piening,¹ Hirale S. Jeevan,¹ Sergey L. Bud'ko,⁴ Paul C. Canfield,⁴ Philipp Gegenwart^{1,3}

2016 © The Authors, some rights reserved; exclusive licensee American Association for the Advancement of Science. Distributed under a Creative Commons Attribution NonCommercial License 4.0 (CC BY-NC). 10.1126/sciadv.1600835

Low-temperature refrigeration is of crucial importance in fundamental research of condensed matter physics, because the investigations of fascinating quantum phenomena, such as superconductivity, superfluidity, and quantum criticality, often require refrigeration down to very low temperatures. Currently, cryogenic refrigerators with ³He gas are widely used for cooling below 1 K. However, usage of the gas has been increasingly difficult because of the current worldwide shortage. Therefore, it is important to consider alternative methods of refrigeration. We show that a new type of refrigerant, the super-heavy electron metal YbCo₂Zn₂₀, can be used for adiabatic demagnetization refrigeration, which does not require ³He gas. This method has a number of advantages, including much better metallic thermal conductivity compared to the conventional insulating refrigerants. We also demonstrate that the cooling performance is optimized in Yb_{1-x}Sc_xCo₂Zn₂₀ by partial Sc substitution, with $x \sim 0.19$. The substitution induces chemical pressure that drives the materials to a zero-field quantum critical point. This leads to an additional enhancement of the magnetocaloric effect in low fields and low temperatures, enabling final temperatures well below 100 mK. This performance has, up to now, been restricted to insulators. For nearly a century, the same principle of using local magnetic moments has been applied for adiabatic demagnetization cooling. This study opens new possibilities of using itinerant magnetic moments for cryogen-free refrigeration.

INTRODUCTION

There have been various reports on the recent ³He crisis due to the increasing imbalance of demand and supply (1–3), which affects a variety of applications, including medical, military, and scientific usages. Demand is rapidly expanded because of the increasing use from various applications, including neutron detectors in homeland security, whereas supply is limited because the gas is produced only through tritium decay in nuclear weapon stockpile and nuclear reactors (1, 2). The increasing demand is becoming unsustainable, leading to a steep rise in price by a factor of more than 10 from 2007 to 2009 (3). This crisis also affects the field of condensed matter physics, because ³He cryogenic refrigerators are most commonly used for cooling below 1 K. Therefore, finding alternative refrigeration techniques is an urgent issue in the field. One of the possible candidates to replace these cryogenic refrigerators is adiabatic demagnetization refrigeration (ADR) (4).

Current ADR for sub-kelvin cooling uses paramagnetic insulators as refrigerants, so-called paramagnetic salts with local magnetic moments (4, 5). At zero field, the moments are randomly oriented, whereas at high fields, the moments are aligned with reduced magnetic entropy (Fig. 1A). When the magnetic field is decreased from high to zero, disordered magnetic moments with increased entropy absorb heat from the lattice, leading to demagnetization cooling. The measure of effectiveness in cooling is magnetocaloric effect (MCE; $\partial T/\partial H|_S$), which quantifies the change of temperature caused by a change of the magnetic field in adiabatic conditions. Paramagnetic salts are widely used because of their large MCE in a temperature range below a few kelvin down to a few tens of millikelvin. However, their poor thermal conductance due to their insulating nature prevents an effective low- T heat transport. The

same holds true for low-dimensional spin chains, tuned toward a quantum critical point (QCP) (see below) (6). Recently, an ADR down to ~ 0.2 K using the metallic compound YbPt₂Sn has been demonstrated (7). In this compound, the magnetic moments of Yb ions, which are responsible for cooling, are fully localized and exhibit a very small mutual interaction. Thus, despite being metallic, it relies on the same principle of operation as that of paramagnetic salts. Furthermore, the coexisting conduction electrons lead to a small but finite Ruderman-Kittel-Kasuya-Yosida (RKKY) interaction, which causes magnetic ordering below 250 mK, preventing cooling to lower temperatures. Since the proposal by P. Debye (8) nearly a century ago, the same principle of using local magnetic moments for ADR has been applied. Below, we show a completely new approach to ADR, which is based on using itinerant magnetic moments in a super-heavy electron (super-HE) metal. Our example demonstrates cooling well below 0.1 K.

An HE state is formed at temperatures below the Kondo temperature T_K through an exchange interaction between f and conduction electrons (9–11). The HE state is easily destroyed by external parameters, such as magnetic field and pressure, owing to its low-energy scale $k_B T_K$. Because the electronic entropy of a metal is proportional to the electronic density of states at the Fermi energy $D(E_F)$ that is proportional to the effective electron mass m^* , the HE state has large entropy (at zero field). This large entropy is suppressed when the HE state is destroyed by applying a magnetic field $\mu_0 H$ of the order $k_B T_K/g\mu_B$ (Fig. 1A). Thus, with decreasing field from high values to zero, a very rapid increase of the entropy is expected. The latter will absorb heat from the lattice system, implying that HE materials can be used for ADR.

HE systems with effective doublet ground state contain a magnetic entropy of $\ln(2)$ above T_K . To optimally use all available magnetic entropy for ADR, the best parameters are the initial temperature $T_i \sim T_K$, the initial field $\mu_0 H_i \sim k_B T_K/g\mu_B = \mu_0 H_K$, and the final field $H_f = 0$. Here, g is the g -factor of conduction electrons. For prototypical HE systems, such as YbRh₂Si₂, both $T_K \sim 25$ K (12) and $\mu_0 H_K \sim 10$ T (13) are too

¹Physikalisches Institut, Georg-August-Universität Göttingen, 37077 Göttingen, Germany. ²Department of Physics, Kyoto University, Kyoto 606-8502, Japan. ³Experimental Physics VI, Center for Electronic Correlations and Magnetism, University of Augsburg, 86159 Augsburg, Germany. ⁴Ames Laboratory, U.S. Department of Energy, and Department of Physics and Astronomy, Iowa State University, Ames, IA 50011, USA. *Corresponding author. Email: yoshifumi.tokiwa@physik.uni-augsburg.de

large for ADR applications that typically require $T_i = 1$ to 2 K and $\mu_0 H_i \leq 8$ T. On the other hand, for Kondo lattice metals with low $T_K \sim 1$ K, typically, the exchange coupling between the moments leads to magnetic ordering, before the full moments are Kondo-screened upon cooling. For Ce-based HE systems, the RKKY interaction is typically of the order 10 K, whereas for Yb-based Kondo metals, it could be weaker. To retain a paramagnetic Kondo-screened state for

an ADR refrigerant material with a low Kondo temperature of only 1 K, a very weak RKKY interaction energy is required. A careful scan of available results in the literature has revealed the most suitable system, $\text{YbCo}_2\text{Zn}_{20}$ (Fig. 1B) (14), which seems to fulfill these severe requirements.

Among all known paramagnetic HE metals, it has one of the lowest Kondo temperatures, $T_K = 1.5$ K (14) (HE metals with this small or even

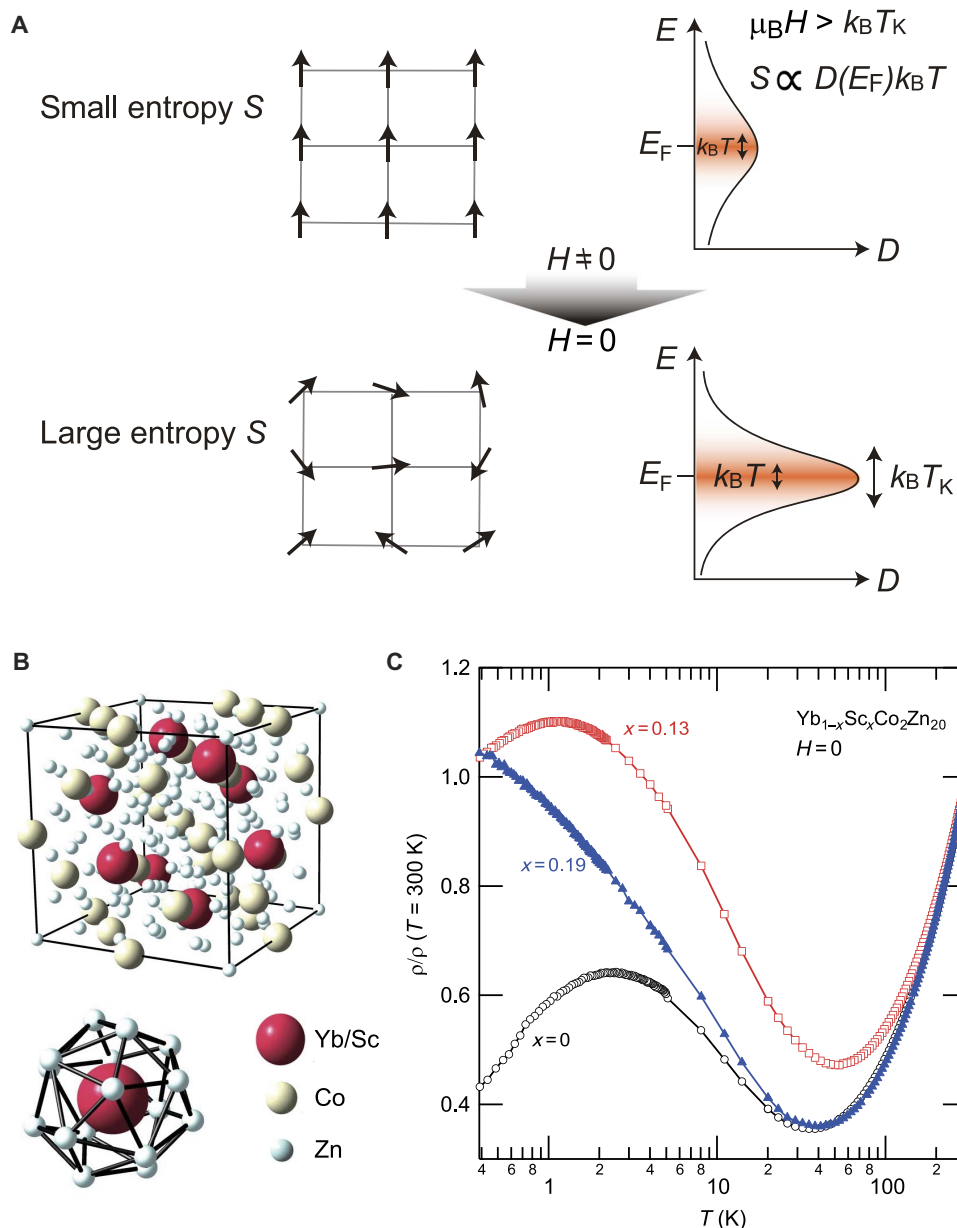


Fig. 1. Adiabatic demagnetization cooling by an HE refrigerant. (A) Comparison of the demagnetization processes for conventional localized moment (left) and HE itinerant moment (right) refrigerants. For the latter (right), the entropy S is proportional to the number of thermally excited holes and electrons, $D(E_F)k_B T$, which corresponds roughly to the area depicted by orange color. Here, D is the density of states. These materials at zero field have a large and sharp peak with a width of $\sim k_B T_K$ in the density of states near E_F . The density of states is being strongly suppressed by the application of fields exceeding $\mu_0 H = k_B T_K / g\mu_B$ (upper right) (14, 28–30), which could be used for adiabatic demagnetization cooling. Note that these are schematic sketches only, and the true $D(E)$ in particular for $H \geq 0$ will display a finer structure. (B) Crystal lattice structure of the super-HE refrigerant $\text{YbCo}_2\text{Zn}_{20}$ and the cage structure of Zn surrounding Yb. (C) Temperature dependence of electrical resistivity at zero field of $\text{Yb}_{1-x}\text{Sc}_x\text{Co}_2\text{Zn}_{20}$, with $x = 0, 0.13,$ and 0.19 .

smaller T_K usually display a long range-ordered ground state). Reflecting the very low T_K , the Kondo coherent state is formed only at very low temperatures, as evidenced by the maximum at 2.5 K in electrical resistivity shown in Fig. 1C. We ascribe the extraordinarily small T_K and T_{RKKY} to its crystal structure, which is the cubic $\text{CeCr}_2\text{Al}_{20}$ type shown in Fig. 1B, consisting of Zn cages surrounding the Yb atoms (14). These cages lead to a very weak hybridization between the Yb 4*f* and the Co 3*d* electrons. This effectively reduces the magnetic exchange interaction J , which enters both T_K and T_{RKKY} . The paramagnetic Fermi liquid (FL) ground state is evidenced by specific heat measurements, which show rapid increases of C/T with decreasing temperature below $T_K = 1.5$ K and saturation at ~ 8 J/mol K² (cf. Fig. 2), one of the largest values among heavy fermion materials (10, 11, 13). This super-HE state is very effectively suppressed by magnetic field, as indicated by the rapid decrease of the T^2 coefficient in electrical resistivity (15). These properties set the system as the most promising candidate for a super-HE refrigerant. It should also be noted that $\text{YbCo}_2\text{Zn}_{20}$ exhibits a field-induced quadrupole ordering for the field only along the [111] direction (16). Because this ordering prevents the rapid decrease of the Sommerfeld coefficient, effective cooling is achieved only when the field is applied away from the [111] direction.

Because the magnetic Grüneisen ratio $\Gamma_H = T^{-1}(\partial T/\partial H)_S$ (which is equal to the adiabatic MCE) diverges at any field-sensitive QCP (17), the

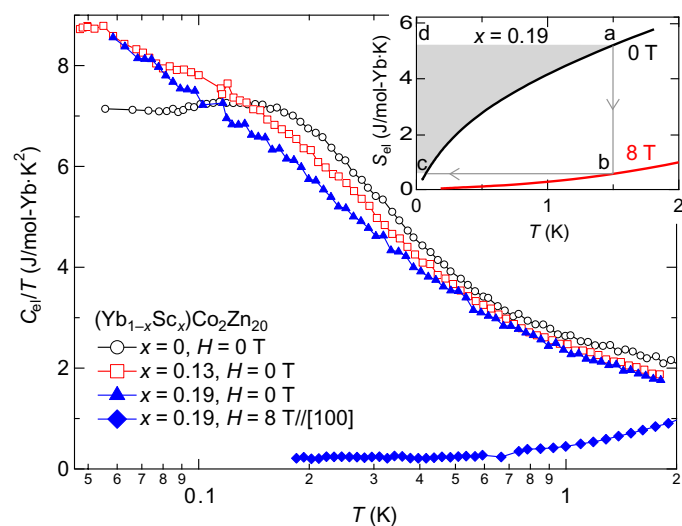


Fig. 2. Formation of the super-HE state in $\text{YbCo}_2\text{Zn}_{20}$ and the diverging effective mass in partially Sc-substituted material. Electronic specific heat divided by temperature C_{el}/T for $H//[100]$ plotted against temperature. The nuclear specific heat was subtracted. C_{el}/T at zero magnetic field for $x = 0, 0.13$, and 0.19 , plotted with black open circles, red open squares, and blue solid triangles, respectively. The data for $x = 0.19$ at a magnetic field of 8 T along the [100] direction are indicated by blue solid diamonds. Inset: The calculated electronic entropy for $x = 0.19$ at zero field and 8 T under the assumption of constant C_{el}/T below the lowest measured temperatures. It is noted that this assumption leads to a slight underestimation of entropy at zero field. The gray lines with arrows indicate the demagnetization cooling process, starting from $\mu_0 H = 8$ T and $T = 1.5$ K. The final temperature T_f is 0.075 K. The gray area indicates the amount of the heat $\Delta Q_c = 2.2$ J/mol, which the material absorbs in the cooling process, whereas the area of rectangle a-b-c-d indicates the heat $\Delta Q_m = 5.6$ J/mol, which is transferred from the material to the heat bath. These yield a high efficiency factor $\Delta Q_m/\Delta Q_c$ of 40%.

usage of quantum critical (QC) materials for ADR was previously proposed (6). It has been reported previously, through measuring electrical resistivity under pressure, that $\text{YbCo}_2\text{Zn}_{20}$ can be tuned to a QCP around 1 GPa, beyond which long-range antiferromagnetic ordering is found (18). We therefore expect that the ADR performance of $\text{YbCo}_2\text{Zn}_{20}$ could be further enhanced when tuning this material toward its QCP. However, for any practical application, the need of applying a hydrostatic pressure leads to severe complications. Therefore, we investigated whether chemical pressure can be used to drive $\text{YbCo}_2\text{Zn}_{20}$ toward quantum criticality, and we found that partial substitution of Yb by the smaller Sc leads to an effective chemical pressure. Below, we investigate the possibility of using the super-HE system $\text{YbCo}_2\text{Zn}_{20}$ for ADR and study also the effect of quantum criticality, induced by chemical pressure, on the cooling performance.

RESULTS

Characterization

Using flux growth (see Materials and Methods), we grew single crystals of $\text{Yb}_{1-x}\text{Sc}_x\text{Co}_2\text{Zn}_{20}$, with $x = 0, 0.13$, and 0.19 . The evolution of the lattice constant follows the Vegard's law, indicating successful substitution of Sc, and the significant lattice contraction with substitution displays a clear chemical pressure effect (see the Supplementary Materials). The temperature dependence of the electrical resistivity of these materials is shown in Fig. 1C. The maximum around 2 K for $x = 0$ indicates the crossover to the coherent Kondo lattice state at low temperatures. In the Sc-substituted material with $x = 0.13$, the resistivity maximum is shifted to lower temperature, suggesting a suppression of T_K by the effect of chemical pressure. Furthermore, the residual resistivity $\rho(T \rightarrow 0)$ is substantially enhanced because of the structural disorder caused by chemical substitution. The resistivity maximum is completely suppressed by further Sc substitution of $x = 0.19$. Here, we note that this enhancement of electrical resistivity would benefit in ADR applications because it reduces eddy current heating in the demagnetization process. The unsubstituted material may not be used for application because of its very high purity, leading to the observation of the de Haas-van Alphen effect (16). We show here that thermal conductivity of Sc-substituted materials is still higher than that of paramagnetic salts. By using the Wiedemann-Franz law (with the resistivity value at the maximum, ~ 70 $\mu\text{ohm}\cdot\text{cm}$), we estimate the smallest electronic thermal conductivity at 50 mK to be 2×10^{-5} W/K cm, which is larger than a typical value of paramagnetic salts, 7×10^{-6} W/K cm (4, 19).

Figure 2 shows the electronic specific heat divided by temperature C_{el}/T of $\text{Yb}_{1-x}\text{Sc}_x\text{Co}_2\text{Zn}_{20}$. The data for $x = 0$ increase logarithmically as temperature is decreased and reach a large constant value of ~ 7 J/mol K² at 0.2 K, indicating the formation of a super-HE state. Chemical pressure by Sc substitution suppresses FL behavior. The heat capacity coefficient for $x = 0.13$ and 0.19 displays further approximately logarithmic increase upon cooling below 0.2 K. This behavior is a signature of quantum criticality, as found in many other HE materials (20). At the lowest measured temperature of 0.05 K, C_{el}/T reaches a value as large as 8.5 J/mol K². Similar to unsubstituted $\text{YbCo}_2\text{Zn}_{20}$ (16), C_{el}/T for $x = 0.19$ is reduced by almost two orders of magnitude by the application of a magnetic field of 8 T. Consequently, the large low-temperature electronic entropy found in zero field is almost completely shifted up to high temperatures by the magnetic field (Fig. 2,

inset). This large entropy difference enables efficient ADR from 1.5 K at 8 T to 0.075 K at 0 T. We note that the difference of entropy is 90% of $R\ln(2)$ in this cooling process, indicating that cooling efficiency cannot be much better in any material, as long as the magnetic entropy of doublet ground states is used. In contrast to paramagnetic salts for which the specific heat follows the high-temperature tail of a Schottky anomaly, $C/T \sim 1/T^3$, and thus rapidly decreases upon warming, $\text{Yb}_{1-x}\text{Sc}_x\text{Co}_2\text{Zn}_{20}$ with the milder $\ln(T)$ dependence displays huge C/T values up to a high temperature of ~ 2 K. As pointed out previously in the context of insulating QC magnets, this large value of specific heat at high temperatures leads to a significantly longer “hold” time compared to paramagnetic salts, which could be of advantage for ADR applications (6).

Quantum criticality of Sc-substituted materials

To compare the performance of the three different samples for ADR, we studied in detail the adiabatic MCE, which is equal to the magnetic Grüneisen parameter $\Gamma_H = T^{-1}(\partial T/\partial H)_S$, using the alternating field method (21). For QC materials, this quantity is expected to display divergent behavior, which has been confirmed for several QC materials recently (17, 22–24). We stress that the nature of a QCP is much more clearly characterized by Γ_H compared to C/T . This is because Γ_H is dominated by the QC contribution with the strongest T dependence, whereas C/T (for example, for antiferromagnetic quantum criticality in three dimensions) is dominated by the noncritical FL contribution, which in our case is extremely large ($\gamma \sim 7$ J/mol K²). Electrical resistivity is also not a good probe of quantum criticality in this study because the resistivity of the Sc-substituted materials has a large residual contribution (Fig. 1C).

Figure 3 shows temperature and magnetic field dependencies on Γ_H for $x = 0, 0.13$, and 0.19 . $\Gamma_H(T)$ for $x = 0$ increases strongly with decreasing temperature and passes through a maximum around 0.5 K. Because $\Gamma_H = -(dM/dT)/C$ (M , magnetization), the nonmonotonic behavior of $\Gamma_H(T)$ for $x = 0$ is probably related to the observed maximum in

magnetic susceptibility at 0.3 K (15). As shown in Fig. 3B, the field dependence of Γ_H for $x = 0$ at $T = 80$ mK changes sign at 0.5 T. This sign change is a typical signature of metamagnetic behavior and is consistent with the previously reported metamagnetism at 0.5 T (15), which is likely ascribed to itinerant moment magnetism, because $4f$ electrons are itinerant in this system. Upon partial substitution of Yb by Sc, the nonmonotonic behaviors in temperature and field dependencies weaken for $x = 0.13$ and completely disappear for $x = 0.19$. $\Gamma_H(T)$ at $\mu_0 H = 0.1$ T for $x = 0.19$ diverges with $T^{-1 \pm 0.05}$ below ~ 0.6 K, and $\Gamma_H(H)$ above $\mu_0 H = 1$ T follows $0.52/\mu_0 H$. The H^{-1} divergence instead of $(H - H_{\text{QCP}})^{-1}$ indicates that the system is tuned exactly to the QCP, with $H_{\text{QCP}} = 0$. The T exponent and the obtained $1/H$ prefactor 0.52 ± 0.03 agree very well with the theoretical prediction for a zero-field QCP of an antiferromagnetic spin density wave (SDW), which yields $\Gamma_H(T, H) \sim H T^{-1}$ in the QC regime and $\Gamma_H(T, H) = 0.5/\mu_0 H$ in the FL regime (17, 24). This theoretical prediction indicates the appearance of a maximum in $\Gamma_H(H)$, corresponding to a crossover field between the QC and the FL regimes, because $\Gamma_H(H) \sim H$ and $\Gamma_H(H) \sim 1/H$ in the former and the latter regimes, respectively. The positions of these maxima are shown by the dotted lines in Fig. 4. For $x = 0.19$, the deviation of $\Gamma_H(H)$ below $\mu_0 H = 1$ T from the expected $1/H$ divergence is caused by the gradual crossover from the FL to the QC regimes with decreasing field. It is intriguing that the system exactly follows the theoretical prediction of an SDW QCP, although it contains significant dilution of magnetic Yb sites. Another likely possibility for causing QC behavior is a quantum Griffiths phase, which is expected in systems with large amounts of disorder. However, the observed critical behavior is incompatible with the Griffiths phase, because theory predicts for this case only a $\log(T)$ dependence in the Grüneisen parameter, which is much weaker than T^{-1} (25).

Detailed measurements of Γ_H are summarized in the color-coded plot, shown in Fig. 4. There appears a small area of negative Γ_H for $x = 0$ because of the sign change in its field dependence. This area of sign change is suppressed with Sc substitution, and monotonic field/temperature dependence is found for $x = 0.19$. The strongest

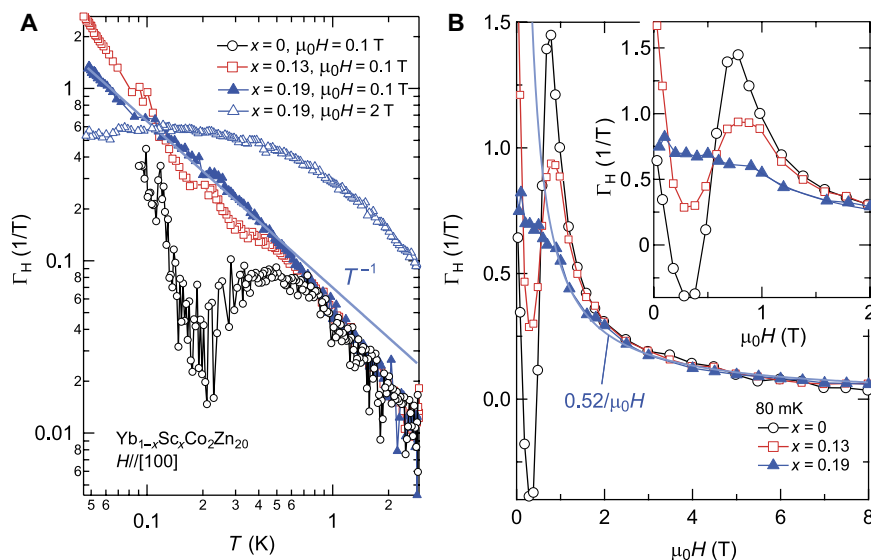


Fig. 3. Tuning to QCP by Sc doping in $\text{Yb}_{1-x}\text{Sc}_x\text{Co}_2\text{Zn}_{20}$. (A) Magnetic Grüneisen ratio Γ_H of $\text{Yb}_{1-x}\text{Sc}_x\text{Co}_2\text{Zn}_{20}$ with $x = 0, 0.13$, and 0.19 as a function of temperature for $H//[100]$. The divergence with a power law $\sim T^{-1}$ for $x = 0.19$ is indicated by the blue solid line. (B) Γ_H at $T = 80$ mK as a function of magnetic field. The solid blue line is a fit to the data for $x = 0.19$ from $\mu_0 H = 1$ to 8 T. Inset: Low-field region.

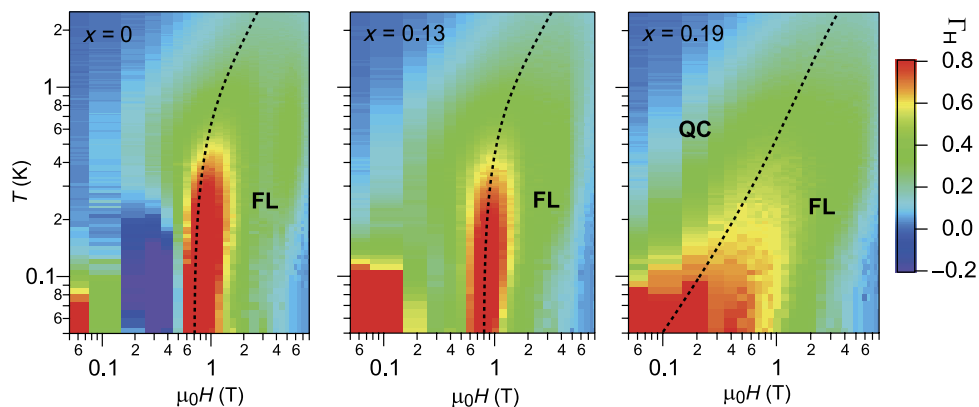


Fig. 4. Visualization of tuning to the QCP by Sc substitution. Color-coded contour plot of the magnetic Grüneisen parameter Γ_H of $\text{Yb}_{1-x}\text{Sc}_x\text{Co}_2\text{Zn}_{20}$ in H - T phase space. Magnetic field has been applied parallel to the [100] direction. Dotted lines indicate maximum positions in the field dependence of $\Gamma_H(H)$. These lines correspond to the crossover field to the FL regime at high fields (24). (See the main text for explanation.) For $x = 0$ and 0.13, the systems at low fields are influenced by quantum fluctuations of metamagnetism around 0.5 T (16), causing a finite-field extrapolation of the maximum position in $\Gamma_H(H)$ for $T \rightarrow 0$. For the critical concentration $x_c = 0.19$, the line is extrapolated to zero, reflecting a zero-field QCP. Γ_H obeys the expected QC behavior of SDW instability, namely, $\Gamma_H(T) \sim 1/T$ in the QC regime and $\Gamma_H(H) \sim 1/H$ in the FL regime (17, 24).

enhancement toward the origin reflects the QCP at zero field for this composition. It is evident that the $x = 0.19$ sample is best suited for ADR toward the zero magnetic field, because the region of highest Γ_H extends toward the origin for this material. We also note that further growth of $\Gamma_H(T)$ upon cooling to even lower temperatures is expected within the QC regime at $H = 0$.

Adiabatic demagnetization cooling by super-HEs

Using these data, we determined the cooling curves under adiabatic conditions (Fig. 5). All the curves display significant cooling effects. The curve for $x = 0.19$ shows a monotonic demagnetization cooling, whereas it is nonmonotonous for the unsubstituted material at low temperatures with a minimum around 0.6 T, which is caused by the metamagnetism (26). When starting from $T_s = 2.5$ K and $\mu_0H_s = 8$ T, the cooling effect for $x = 0$ is slightly better than that for $x = 0.13$ and 0.19, with a lower final temperature at zero field (T_f). Starting from $T_i = 1$ K, T_f becomes slightly lower with steeper slope at low temperature for $x = 0.13$ and 0.19 than that for $x = 0$. As shown in the inset of Fig. 2, a steeper slope of entropy, which is equal to C/T , leads to a lower final temperature. Because C/T is larger for $x = 0.13$ and 0.19 than for $x = 0$ below $T \sim 100$ mK, better cooling due to the QCP is realized at very low temperatures. We point out that C/T may diverge toward zero temperature at the QCP. Thus, cooling to arbitrary low temperatures may be possible because of the significant $dS/dT = C/T$, even in the limit of zero temperature. For $x = 0.19$, the final temperature reaches the lower limit of our experimental setup, which is 40 mK, when we set the initial temperature to a low value $T_i = 1$ K.

DISCUSSION

Here, we show that the HE metallic system $\text{Yb}_{1-x}\text{Sc}_x\text{Co}_2\text{Zn}_{20}$ can be used as a new type of refrigerant for ADR with itinerant magnetic moments. The steep increase of entropy due to the diverging C/T in the QC Sc-substituted material (Fig. 2) enables cooling down to temperatures even lower than the lowest temperature of our experimental setup, which is 40 mK. These results, along with the usage of most of the avail-

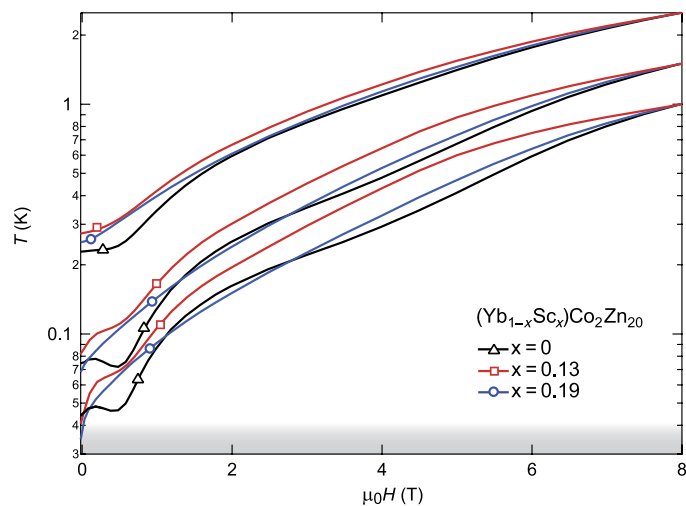


Fig. 5. Adiabatic demagnetization refrigeration of $\text{Yb}_{1-x}\text{Sc}_x\text{Co}_2\text{Zn}_{20}$. Solid black, red, and blue curves represent the cooling curves for $x = 0, 0.13,$ and 0.19, respectively. The curves are obtained by integrating the MCE ($\partial T/\partial H|_S$) from 8 T to zero field. Magnetic field is applied parallel to the [100] direction. The points at low temperature below the lower limit of the thermometer calibration (40 mK) are obtained by extrapolating the calibration data. The out-of-calibration range is shaded by gray.

able magnetic entropy $R \ln(2)$ (Fig. 2, inset), indicate that the QC Sc-substituted $\text{YbCo}_2\text{Zn}_{20}$ is an ideal metallic refrigerant. HE metallic refrigerants have major advantages compared to insulating paramagnetic salts, such as an additional electronic thermal conductivity, stability in the air, and easy machining, because they are much less brittle compared to salts. In the conventional ADR systems, large amounts of Cu or Ag wires are spread uniformly in the paramagnetic salt pill to improve thermal conductance (4). One possible immediate application may be replacing the metallic wires with $\text{YbCo}_2\text{Zn}_{20}$, which would strongly improve the cooling performance. Thus, the HE refrigerants provide realistic possibilities of application and even replacement for conventional paramagnetic salts.

MATERIALS AND METHODS

Single crystals of $\text{Yb}_{1-x}\text{Sc}_x\text{Co}_2\text{Zn}_{20}$ were grown by the self-flux method (14, 27). The compositions of obtained crystals were determined by energy-dispersive x-ray analysis.

Electrical resistivity was measured using the standard four-probe technique. Single crystals of $\text{Yb}_{1-x}\text{Sc}_x\text{Co}_2\text{Zn}_{20}$ with a dimension of $\sim 2 \times 2 \times 0.5 \text{ mm}^3$ were used for specific heat and MCE experiments. The specific heat was measured by the standard quasi-adiabatic heat pulse method, using a dilution refrigerator.

The MCE was measured by using an alternating field technique adapted to a dilution refrigerator (21). We varied frequency (f) for the alternating field, depending on the temperature. The sample is in a quasi-adiabatic condition with a weak heat link to the bath, causing T -dependent relaxation time τ , which increases with decreasing T . To ensure the effective adiabatic condition for MCE measurements, it is necessary to maintain a condition, $f \gg 1/\tau$. We also point out that the relaxation time between the sample and thermometer (τ') becomes longer with decreasing T , leading to the other necessary condition— $f \ll 1/\tau'$. Thus, one needs to maintain $\tau' \gg 1/f \gg \tau$. This is easily checked by measuring the f dependence of the MCE signal. If the condition is maintained, the signal is f -independent. We obtained f -independent MCE signal for each measurement. Typically, we use 0.1 Hz at high temperatures above 1 K and 0.02 Hz at low temperatures below 0.2 K. This ensures perfect adiabatic conditions. Thus, our data of the MCE are identical to the magnetic Grüneisen parameter. We also changed the amplitude of the alternating field. Because the magnetic Grüneisen parameter becomes very sensitive to the field at low temperatures, we decreased the amplitude with decreasing temperature. We decrease it from 0.02 T at temperatures above 1 K to 0.004 T at temperatures below 0.2 K.

SUPPLEMENTARY MATERIALS

Supplementary material for this article is available at <http://advances.sciencemag.org/cgi/content/full/2/9/e1600835/DC1>

fig. S1. Sc substitution dependence of lattice constant a .

REFERENCES AND NOTES

- D. A. Shea, D. Morgan, "The helium-3 shortage: Supply, demand, and options for congress" (Report R41419, Congressional Research Service, 2010); www.fas.org/sgp/crs/misc/R41419.pdf.
- R. T. Kouzes, J. H. Ely, "Status summary of ^3He and neutron detection alternatives for homeland security" (Report PNNL-19360, Pacific Northwest National Laboratory, 2010); www.pnl.gov/main/publications/external/technical_reports/PNNL-19360.pdf.
- A. Cho, Helium-3 shortage could put freeze on low-temperature research. *Science* **326**, 778–779 (2009).
- F. Pobell, *Matter and Methods at Low Temperatures* (Springer-Verlag Berlin, Heidelberg, Berlin, 1992).
- O. E. Vilches, J. C. Wheatley, Measurements of the specific heats of three magnetic salts at low temperatures. *Phys. Rev.* **148**, 509–516 (1966).
- B. Wolf, Y. Tsui, D. Jaiswal-Nagar, U. Tutsch, A. Honecker, K. Remović-Langer, G. Hofmann, A. Prokofiev, W. Assmus, G. Donath, M. Lang, Magnetocaloric effect and magnetic cooling near a field-induced quantum-critical point. *Proc. Natl. Acad. Sci. U.S.A.* **108**, 6862–6866 (2011).
- D. Jang, T. Gruner, A. Steppke, K. Mitsumoto, C. Geibel, M. Brando, Large magnetocaloric effect and adiabatic demagnetization refrigeration with YbPt_2Sn . *Nat. Commun.* **6**, 8680 (2015).
- P. Debye, Einige Bemerkungen zur Magnetisierung bei tiefer Temperatur. *Ann. Phys.* **386**, 1154–1160 (1926).
- G. R. Stewart, Heavy-fermion systems. *Rev. Mod. Phys.* **56**, 755 (1984).
- Z. Fisk, J. L. Sarrao, J. L. Smith, J. D. Thompson, The physics and chemistry of heavy fermions. *Proc. Natl. Acad. Sci. U.S.A.* **92**, 6663–6667 (1995).
- A. C. Hewson, *The Kondo Problem to Heavy Fermions* (Cambridge Univ. Press, Cambridge, 2003).
- O. Trovarelli, C. Geibel, S. Mederle, C. Langhammer, F. M. Grosche, P. Gegenwart, M. Lang, G. Sparr, F. Steglich, YbRh_2Si_2 : Pronounced non-fermi-liquid effects above a low-lying magnetic phase transition. *Phys. Rev. Lett.* **85**, 626–629 (2000).
- Y. Tokiwa, P. Gegenwart, T. Radu, J. Ferstl, G. Sparr, C. Geibel, F. Steglich, Field-induced suppression of the heavy-fermion state in YbRh_2Si_2 . *Phys. Rev. Lett.* **94**, 226402 (2005).
- M. S. Torikachvili, S. Jia, E. D. Mun, S. T. Hannahs, R. C. Black, W. K. Neils, D. Martien, S. L. Bud'ko, P. C. Canfield, Six closely related $\text{YbT}_2\text{Zn}_{20}$ ($T = \text{Fe, Co, Ru, Rh, Os, Ir}$) heavy fermion compounds with large local moment degeneracy. *Proc. Natl. Acad. Sci. U.S.A.* **104**, 9960–9963 (2007).
- M. Ohya, M. Matsushita, S. Yoshiuchi, T. Takeuchi, F. Honda, R. Settai, T. Tanaka, Y. Kubo, Y. Ōnuki, Strong field quenching of the quasiparticle effective mass in heavy fermion compound $\text{YbCo}_2\text{Zn}_{20}$. *J. Phys. Soc. Jpn.* **79**, 083601 (2010).
- T. Takeuchi, S. Yoshiuchi, M. Ohya, Y. Taga, Y. Hirose, K. Sugiyama, F. Honda, M. Hagiwara, K. Kindo, R. Settai, Y. Ōnuki, Field-induced quadrupolar ordered phase for $||\langle 111 \rangle|$ in heavy-fermion compound $\text{YbCo}_2\text{Zn}_{20}$. *J. Phys. Soc. Jpn.* **80**, 114703 (2011).
- L. Zhu, M. Garst, A. Rosch, Q. Si, Universally diverging Grüneisen parameter and the magnetocaloric effect close to quantum critical points. *Phys. Rev. Lett.* **91**, 066404 (2003).
- Y. Saiga, K. Matsubayashi, T. Fujiwara, M. Kosaka, S. Katano, M. Hedo, T. Matsumoto, Y. Uwatoko, Pressure-induced magnetic transition in a single crystal of $\text{YbCo}_2\text{Zn}_{20}$. *J. Phys. Soc. Jpn.* **77**, 053710 (2008).
- C. G. B. Garrett, The thermal conductivity of potassium chrome alum at temperatures below one degree absolute. *Philos. Mag.* **41**, 621–630 (1950).
- H. v. Löhneysen, A. Rosch, M. Vojta, P. Wölfle, Fermi-liquid instabilities at magnetic quantum phase transitions. *Rev. Mod. Phys.* **79**, 1015–1075 (2007).
- Y. Tokiwa, P. Gegenwart, High-resolution alternating-field technique to determine the magnetocaloric effect of metals down to very low temperatures. *Rev. Sci. Instrum.* **82**, 013905 (2011).
- M. Garst, A. Rosch, Sign change of the Grüneisen parameter and magnetocaloric effect near quantum critical points. *Phys. Rev. B* **72**, 205129 (2005).
- Y. Tokiwa, T. Radu, C. Geibel, F. Steglich, P. Gegenwart, Divergence of the magnetic Grüneisen ratio at the field-induced quantum critical point in YbRh_2Si_2 . *Phys. Rev. Lett.* **102**, 066401 (2009).
- Y. Tokiwa, E. D. Bauer, P. Gegenwart, Zero-field quantum critical point in CeCoIn_5 . *Phys. Rev. Lett.* **111**, 107003 (2013).
- T. Vojta, Thermal expansion and Grüneisen parameter in quantum Griffiths phases. *Phys. Rev. B* **80**, 041101(R) (2009).
- Y. Hirose, M. Toda, S. Yoshiuchi, S. Yasui, K. Sugiyama, F. Honda, M. Hagiwara, K. Kindo, R. Settai, Y. Ōnuki, Metamagnetic transition in heavy fermion compounds $\text{YbT}_2\text{Zn}_{20}$ ($T = \text{Co, Rh, Ir}$). *J. Phys. Conf. Ser.* **273**, 012003 (2011).
- P. C. Canfield, Z. Fisk, Growth of single crystals from metallic fluxes. *Philos. Mag.* **65**, 1117–1123 (1992).
- J. Custers, P. Gegenwart, H. Wilhelm, K. Neumaier, Y. Tokiwa, O. Trovarelli, C. Geibel, F. Steglich, C. Pépin, P. Coleman, The break-up of heavy electrons at a quantum critical point. *Nature* **424**, 524–527 (2003).
- A. Bianchi, R. Movshovich, I. Vekhter, P. G. Pagliuso, J. L. Sarrao, Avoided antiferromagnetic order and quantum critical point in CeCoIn_5 . *Phys. Rev. Lett.* **91**, 257001 (2003).
- J. Paglione, M. A. Tanatar, D. G. Hawthorn, E. Boaknin, R. W. Hill, F. Ronning, M. Sutherland, L. Taillefer, C. Petrovic, P. C. Canfield, Field-induced quantum critical point in CeCoIn_5 . *Phys. Rev. Lett.* **91**, 246405 (2003).

Acknowledgments

Funding: Financial support for this work was provided by the German Science Foundation and the Grants-in-Aid for Scientific Research (no. 15K13521) from the Japan Society for the Promotion of Science. Part of this research was performed by P.C.C. and S.L.B. at the Ames Laboratory and supported by the Division of Materials Sciences and Engineering, Office of Basic Energy Science, U.S. Department of Energy. Ames Laboratory is operated for the U.S. Department of Energy by Iowa State University under contract no. DE-AC02-07CH11358. **Author contributions:** P.G. conceived the project. Y.T. and P.G. planned and designed the experiments. Y.T. and B.P. performed the measurements. B.P., H.S.J., S.L.B., and P.C.C. synthesized and characterized the samples. Y.T. and P.G. discussed the results and prepared the manuscript. **Competing interests:** The authors declare that they have no competing interests. **Data and materials availability:** All data needed to evaluate the conclusions in the paper are present in the paper and/or the Supplementary Materials. Additional data related to this paper may be requested from the authors.

Submitted 20 April 2016

Accepted 9 August 2016

Published 9 September 2016

10.1126/sciadv.1600835

Citation: Y. Tokiwa, B. Piening, H. S. Jeevan, S. L. Bud'ko, P. C. Canfield, P. Gegenwart, Super-heavy electron material as metallic refrigerant for adiabatic demagnetization cooling. *Sci. Adv.* **2**, e1600835 (2016).

Super-heavy electron material as metallic refrigerant for adiabatic demagnetization cooling

Yoshifumi Tokiwa, Boy Piening, Hirale S. Jeevan, Sergey L. Bud'ko, Paul C. Canfield and Philipp Gegenwart

Sci Adv 2 (9), e1600835.

DOI: 10.1126/sciadv.1600835

ARTICLE TOOLS

<http://advances.sciencemag.org/content/2/9/e1600835>

SUPPLEMENTARY MATERIALS

<http://advances.sciencemag.org/content/suppl/2016/09/06/2.9.e1600835.DC1>

REFERENCES

This article cites 26 articles, 4 of which you can access for free
<http://advances.sciencemag.org/content/2/9/e1600835#BIBL>

PERMISSIONS

<http://www.sciencemag.org/help/reprints-and-permissions>

Use of this article is subject to the [Terms of Service](#)

Science Advances (ISSN 2375-2548) is published by the American Association for the Advancement of Science, 1200 New York Avenue NW, Washington, DC 20005. 2017 © The Authors, some rights reserved; exclusive licensee American Association for the Advancement of Science. No claim to original U.S. Government Works. The title *Science Advances* is a registered trademark of AAAS.